Event-based Multisensor Fusion with Correlated Estimates

Eva Julia Schmitt and Benjamin Noack
Autonomous Multisensor Systems Group
Institute for Intelligent Cooperating Systems
Otto von Guericke University Magdeburg, Germany
eva.schmitt@ovgu.de, benjamin.noack@ieee.org

***Abstract*—Many automation tasks require to fuse information that is acquired by distributed sensors and passed through a wireless network across multiple nodes. The growing number of connected sensors and agents increases the burden on the communications network and the energy consumption. Further challenges in information fusion arise from correlated data shared between nodes. To mitigate the negative effects, an efficient multi-sensor fusion approach is presented in this paper. A system design that uses stochastic event-based instead of periodic transmissions is proposed based on two different algorithms, the augmented state approach and fast covariance intersection. Furthermore, two different network topologies are investigated and a methodology to handle correlations among both finite impulse response and recursive estimates is developed. Together, the results represent a wide range of network topologies and possible correlation structures and give insights into the estimation performance and network utilization.**

***Index Terms*—Multisensor fusion, event-based estimation, correlated inputs**

I. Introduction

The increasing automation and interaction of agents in many fields such as automated driving and IoT 4.0 applications, e. g. smart manufacturing, smart farming and smart cities [1], [2], require a large number of sensors to be deployed to observe the environment and to enable decision-making, control and optimization. These sensors are often organized in networks and share information among each other and agents in their vicinity frequently via wireless communications. As the number of sensors and agents in an environment increases, the burden on the communications network grows simultaneously. In this regard, event-based transmissions and state estimation can help to utilize the communications resources efficiently. The idea behind event-based transmissions is to transmit data only if relevant information is available at the transmitter rather than periodically in fixed time intervals. The relevance of the information is determined using a triggering condition that is known to the transmitting and the receiving node. Stochastic event-triggers with matching estimators that use implicit information in non-transmission instants are of particular interest due to their beneficial properties such as the preservation of the Gaussianity of the state variable and the intuitive yet efficient estimator design. Several variants of stochastic triggering have been proposed in [3]–[5].

Multisensor systems typically fuse information from different sources. Often many nodes perform state estimations of an underlying physical process, e. g., the movement of an agent. Thus, the resulting estimates can be correlated through the observed common process noise. Depending on the topology of the network, also estimates correlated in time may have to be fused to obtain the best possible output. Different fusion methods have been proposed in the past, e. g., covariance intersection [6], the Bar-Shalom-Campo formula [7] or tracklet fusion [8]. Furthermore, several estimators for handling inputs with correlated noise like the augmented state (AS) approach and the state differencing method [9], and the colored-noise Kalman filter [10] have been developed. All of the previously mentioned methods have different strengths and limitations.

In this work, we focus on the AS approach and fast covariance intersection (FCI) [11] and extend both to handle event-based transmissions in multisensor systems. Advantages of the AS approach lie in its optimality regarding the provided information, the flexibility to handle many different correlation structures and sensor topologies as well as its simplicity by avoiding the calculation of crosscorrelations between sensor nodes. However, the approach did not find much attention in the past due to its increased computational complexity and possible singularities in the calculation of the Kalman gain. As will be shown in the course of the paper, the drawbacks can be mitigated in the intended application. FCI is used as a second approach due to its simplicity and broad applicability by not requiring any information on the correlation structure of different estimates. However, due to the conservativeness of the approach, FCI generally returns suboptimal results.

The contributions can be summarized as follows: Two different event-based estimators for multisensor fusion with correlated estimates are developed, one based on the AS approach, the other one based on FCI. Both are investigated under periodic and stochastic event-based transmissions. Two base network topologies are considered, the star and the chain topology, which can be combined to obtain a large variety of topologies. In case of the star topology, heterogeneous smart sensors that use a finite impulse response (FIR) filter or Kalman filter (KF) for local state estimation are considered to show the effectiveness of the approach to fuse finite time and recursively correlated estimates at the fusion center. For the chain topology, solely KF sensors are used due to their optimality. With the help of numerical simulations the two algorithms are compared and the network utilization is analyzed.

II. Notation

An underlined variable $\underline{x} \in \mathbb{R}^q$ denotes a real-valued vector. Lowercase boldface letters $\underline{\mathbf{x}}$ are used for quantities with random components. Matrices are written in uppercase boldface letters $\mathbf{C} \in \mathbb{R}^{q\times q}$, and $\mathbf{C}^{-1}$ and $\mathbf{C}^{\mathrm{T}}$ are its inverse and transpose, respectively. $\mathbf{0}_{p\times q}$ is the zero matrix with p rows and q columns. $\mathbf{0}_p \in \mathbb{R}^{p\times p}$ or $\mathbf{I}_p \in \mathbb{R}^{p\times p}$ are the zero or identity square matrices, respectively. The notation $\underline{\hat{\mathbf{x}}}_{k|k-l}$ denotes an estimate at time step k conditioned on measurements up to time step $k-l$. Matrix inequalities $\mathbf{A} \geq \mathbf{B}$ are defined such that $\mathbf{A} - \mathbf{B}$ is positive semidefinite.

III. Stochastic Event-based Triggering and Estimation

Before presenting the novel algorithms for event-based multisensor fusion, the used system model and basics of stochastic event-based triggering and estimation will be reviewed.

A. System model

A system consisting of multiple sensors $i = 1, \dots, N$ monitoring a physical process, a triggering unit located at each of the sensors and a remote receiver with a state estimator to reconstruct the physical process is considered. The state and the measurement equation of the observed process are given by the discrete-time linear system

$$\begin{aligned} \underline{\mathbf{x}}_{k+1} &= \mathbf{A}\,\underline{\mathbf{x}}_k + \underline{\mathbf{w}}_k\,, \\ \underline{\mathbf{y}}^i_k &= \mathbf{C}^i\,\underline{\mathbf{x}}_k + \underline{\mathbf{v}}^i_k\,, \end{aligned}$$

where $\underline{\mathbf{x}}_k \in \mathbb{R}^{n_x}$ is the state at time step $k \in \mathbb{N}$, and $\underline{\mathbf{y}}^i_k \in \mathbb{R}^{n^i_y}$ denote the observations. The time-invariant process and measurement matrices are given by $\mathbf{A} \in \mathbb{R}^{n_x\times n_x}$ and $\mathbf{C}^i \in \mathbb{R}^{n^i_y\times n_x}$, respectively. The process noise $\underline{\mathbf{w}}_l \sim \mathcal{N}(\underline{0}, \mathbf{Q})$ and measurement noise $\underline{\mathbf{v}}^i_m \sim \mathcal{N}(\underline{0}, \mathbf{R}^i)$ are white and mutually uncorrelated for arbitrary $l, m \in \mathbb{N}$. Also, measurements $\underline{\mathbf{v}}^i_k$, $\underline{\mathbf{v}}^j_k$ from different sensors are uncorrelated for $i \neq j \in \mathbb{N}$. When only one sensor is considered, the superscript i is omitted. Further, detectability and stabilizability are assumed:

Assumption 1. The pair $(\mathbf{A}, \mathbf{C})$ is detectable and the pair $(\mathbf{A}, \mathbf{G})$ with $\mathbf{G}\mathbf{G}^{\mathrm{T}} = \mathbf{Q}$ is stabilizable.

B. Stochastic Event-triggering

Stochastic event-triggers with an innovation-like triggering variable $\underline{\mathbf{z}}_k = \underline{\mathbf{y}}_k - \underline{c}_k$ with arbitrary $\underline{c}_k \in \mathbb{R}^{n_y}$ are considered. In the following, a short overview of stochastic event-triggers and matching estimators is given. For further details, the reader is referred to [3]–[5].

A decision variable γ_k and an according decision scheme

$$\gamma_k = \begin{cases} 1, & \boldsymbol{\xi}_k > \phi(\underline{\mathbf{z}}_k)\,, \\ 0, & \boldsymbol{\xi}_k \leq \phi(\underline{\mathbf{z}}_k)\,, \end{cases} \tag{1}$$

are defined such that $\gamma_k = 1$ implies that an event has been triggered in time instant k. $\boldsymbol{\xi}_k$ is an instance of an independent and identically distributed random variable uniformly distributed between 0 and 1, and $\phi(\underline{\mathbf{z}}_k) = \exp\left(-\frac{1}{2}\,(\underline{\mathbf{y}}_k - \underline{c}_k)^{\mathrm{T}}\,\mathbf{Z}^{-1}\,(\underline{\mathbf{y}}_k - \underline{c}_k)\right)$ has a form similar to a Gaussian distribution. The design variable $\mathbf{Z}_k \in \mathbb{R}^{n_y\times n_y}$ is used to control the transmission frequency, where high values of $\mathbf{Z}$ lead to a low transmission probability.

The transmission probability conditioned on $\underline{\mathbf{y}}_k$ is given by

$$\begin{aligned} \Pr\{\gamma_k = 1 \,|\, \underline{\mathbf{y}}_k\} &= 1 - \phi(\underline{\mathbf{y}}_k - \underline{c}_k)\,, \\ \Pr\{\gamma_k = 0 \,|\, \underline{\mathbf{y}}_k\} &= \phi(\underline{\mathbf{y}}_k - \underline{c}_k)\,. \end{aligned}$$

C. Matching estimator

As presented in [5], an estimator matching the class of innovation-based stochastic triggers that uses implicit measurements in non-transmission instants can be derived from the standard KF formulation. The prediction step for the state estimate $\underline{\hat{\mathbf{x}}}_{k|k}$ and estimation error covariance $\mathbf{P}_{k|k}$

$$\begin{aligned} \underline{\hat{\mathbf{x}}}_{k|k-1} &= \mathbf{A}\,\underline{\hat{\mathbf{x}}}_{k-1|k-1}\,, \\ \mathbf{P}_{k|k-1} &= \mathbf{A}\,\mathbf{P}_{k-1|k-1}\,\mathbf{A}^{\mathrm{T}} + \mathbf{Q} \end{aligned}$$

is not altered, whereas the update step is given by

$$\begin{aligned} \underline{\hat{\mathbf{x}}}_{k|k} &= \underline{\hat{\mathbf{x}}}_{k|k-1} - \mathbf{K}_k\,(\gamma_k\,\underline{\mathbf{z}}_k - \underline{\hat{\mathbf{z}}}_{k|k-1})\,, \\ \underline{\mathbf{z}}_k &= \underline{\mathbf{y}}_k - \underline{c}_k\,, \quad \underline{\hat{\mathbf{z}}}_{k|k-1} = \mathbf{C}\,\underline{\hat{\mathbf{x}}}_{k|k-1} - \underline{c}_k\,, \\ \mathbf{P}_{k|k} &= \left(\mathbf{I}_{n_x} - \mathbf{K}_k\,\mathbf{C}\right)\mathbf{P}_{k|k-1}\,, \end{aligned}$$

with the Kalman gain

$$\mathbf{K}_k = \mathbf{P}_{k|k-1}\,\mathbf{C}^{\mathrm{T}}\Big(\mathbf{C}\mathbf{P}_{k|k-1}\,\mathbf{C}^{\mathrm{T}} + \mathbf{R} + (1-\gamma_k)\mathbf{Z}\Big)^{-1}.$$

For $\gamma_k = 1$, $\underline{c}_k$ and $\mathbf{Z}$ vanish and the above equations reduce to those of the standard KF. For $\gamma_k = 0$, the implicit measurement $\underline{c}_k = \mathbf{C}\,\underline{\mathbf{x}}_k + \underline{\mathbf{v}}_k + \underline{\boldsymbol{\eta}}_k$ with $\underline{\mathbf{v}}_k + \underline{\boldsymbol{\eta}}_k \sim \mathcal{N}(\underline{0}, \mathbf{R} + \mathbf{Z})$ is used, which is justified in Theorem 1.

Theorem 1. For $\gamma_k = 0$, $\underline{c}_k$ serves as an implicit measurement with $\underline{c}_k = \mathbf{C}\,\underline{\mathbf{x}}_k + \underline{\mathbf{v}}_k + \underline{\boldsymbol{\eta}}_k$. The noise component $\underline{\boldsymbol{\eta}}_k$ introduced by the event-triggering condition is an additional additive white Gaussian noise (AWGN) measurement noise with $\underline{\boldsymbol{\eta}}_k \sim \mathcal{N}(\underline{\mathbf{0}}, \mathbf{Z})$.

Proof. The proof follows from the proof for the free choice of $\underline{c}_k$ in the appendix of [5]. The case $\gamma_k = 0$ is considered:

$$\begin{aligned} \Pr\left\{\gamma_k = 0 \,\middle|\, \underline{\mathbf{x}}_k\right\} &= \int_{-\infty}^{\infty} \Pr\left\{\gamma_k = 0, \underline{\mathbf{y}}_k \,\middle|\, \underline{\mathbf{x}}_k\right\} \mathrm{d}\,\underline{\mathbf{y}}_k \\ &\propto \exp\left(-0.5(\underline{c}_k - \mathbf{C}\,\underline{\mathbf{x}}_k)^{\mathrm{T}}(\mathbf{Z} + \mathbf{R})^{-1}(\underline{c}_k - \mathbf{C}\,\underline{\mathbf{x}}_k)\right)\,. \end{aligned}$$

Hence, this likelihood encodes the implicit measurement $\underline{c}_k = \mathbf{C}\,\underline{\mathbf{x}}_k + \underline{\mathbf{v}}_k + \underline{\boldsymbol{\eta}}_k$. In the special case $\mathbf{R} = \mathbf{0}_{n_y}$, it holds

$$\begin{aligned} &\Pr\left\{\gamma_k = 0 \middle| \underline{\mathbf{x}}_k\right\} \propto \int_{-\infty}^{\infty} \exp\left(-0.5(\underline{\mathbf{y}}_k - \underline{c}_k)^{\mathrm{T}}\,\mathbf{Z}^{-1}\,(\underline{\mathbf{y}}_k - \underline{c}_k)\right) \\ &\cdot \delta(y - \mathbf{C}\underline{\mathbf{x}}_k)\,\mathrm{d}\,\underline{\mathbf{y}}_k \\ &= \exp\left(-0.5(\underline{c}_k - \mathbf{C}\underline{\mathbf{x}}_k)^{\mathrm{T}}\mathbf{Z}^{-1}(\underline{c}_k - \mathbf{C}\underline{\mathbf{x}}_k)\right). \end{aligned}$$

□

D. Event-based Procedure and Resulting Challenges

The event-based procedure with a stochastic trigger can be summarized as follows.

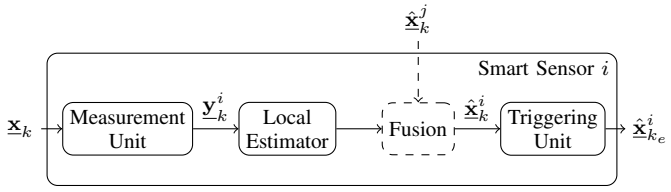

Fig. 1: Smart sensor with optional fusion.

1) $\gamma_k = 1$*:* An event is triggered at the sensor and the current measurement $\underline{\mathbf{y}}_{k_e}$ along with $\underline{c}_{k_e}$ is transmitted to the receiving remote estimator. The remote estimator performs a filtering step with the received measurement.

2) $\gamma_k = 0$*:* Both, sensor and receiver use the same rule to determine $\underline{c}_k$ from $\underline{c}_{k_e}$ of the last event instant. If calculating $\underline{\mathbf{z}}_k$ and inserting it into (1) leads to $\gamma_k = 0$, no new event is triggered at the sensor. Hence, the estimator at the receiver has to perform an update with the implicit measurement $\underline{c}_k$.

The matching estimator as described in III-C can only be applied directly, if measurements $\underline{\mathbf{y}}_k$ with uncorrelated noise terms are used in the triggering condition. If a smart sensor is employed that uses local state estimates instead of raw measurements in its triggering condition and for transmission, this generally leads to better results regarding the transmission frequency versus estimation performance trade-off. However, such estimates are correlated in time and suitable fusion techniques need to be found to include them in the event-based state estimation in single- and multisensor scenarios. The structure of the proposed smart sensors and the correlation structure of the resulting outputs are introduced next.

E. Smart Sensors

In this paper, a smart sensor i as shown in Fig. 1 is comprised of a measurement unit that observes a physical process, a model-based local estimator that processes local measurements, an optional fusion instance to fuse own estimates and estimates from possible neighboring nodes j and a stochastic event-based triggering unit. Within this work, two different types of smart sensors producing time-correlated data are considered that cover a large set of possible correlations: finite-time and recursive correlations. The first sensor type uses an FIR estimator, the second sensor type uses a KF. Both employ a stochastic send-on-delta with prediction trigger [5] with a triggering variable of the form $\underline{\mathbf{z}}_k = \hat{\underline{\mathbf{x}}}_{k|k} - \mathbf{A}^{k-k_e}\hat{\underline{\mathbf{x}}}_{k_e|k_e}$. The triggering condition implies that the explicit and implicit information has the correlation structure of $\hat{\underline{\mathbf{x}}}_{k|k}$. Since the sensors' state estimates shall be used as state measurements at the receiving node, their error terms need to be investigated.

1) FIR Estimates: The FIR estimator using the stacked last m measurements $\underline{\mathbf{y}}_{\text{last}}$ is given by

$$\hat{\underline{\mathbf{x}}}_k^{\text{FIR}} = \left(\boldsymbol{\mathcal{H}}^{\text{T}}\,\mathbf{N}^{-1}\,\boldsymbol{\mathcal{H}}\right)^{-1}\boldsymbol{\mathcal{H}}^{\text{T}}\,\mathbf{N}^{-1}\,\underline{\mathbf{y}}_{\text{last}}\,.$$

Its error can be characterized by

$$\underline{\mathbf{e}}_k = \hat{\underline{\mathbf{x}}}_k^{\text{FIR}} - \underline{\mathbf{x}}_k = \left(\boldsymbol{\mathcal{H}}^{\text{T}}\,\mathbf{N}^{-1}\,\boldsymbol{\mathcal{H}}\right)^{-1}\boldsymbol{\mathcal{H}}^{\text{T}}\,\mathbf{N}^{-1}\underline{\mathbf{n}}_k$$

with the corresponding error covariance matrix

$$\mathbf{E} = \text{Cov}\left\{\tilde{\underline{\boldsymbol{x}}}_k^{\text{FIR}}\right\} = \left(\boldsymbol{\mathcal{H}}^{\text{T}}\,\mathbf{N}^{-1}\,\boldsymbol{\mathcal{H}}\right)^{-1},$$

where $\boldsymbol{\mathcal{H}}\,, \mathbf{N}, \underline{\mathbf{n}}_k$ are defined in [12], [13].

2) KF Estimates: Due to the recursive nature of the KF, also the error of the KF can be represented recursively by

$$\begin{aligned}\tilde{\underline{\mathbf{x}}}_k &= \hat{\underline{\mathbf{x}}}_k - \underline{\mathbf{x}}_k \\ &= (\mathbf{I}_{n_x} - \mathbf{K}_k\mathbf{C})\mathbf{A}\tilde{\underline{\mathbf{x}}}_{k-1} - (\mathbf{I}_{n_x} - \mathbf{K}_k\mathbf{C})\underline{\mathbf{w}}_{k-1} + \mathbf{K}_k\underline{\mathbf{v}}_k \\ &= \psi_k\tilde{\underline{\mathbf{x}}}_{k-1} + \alpha_k\underline{\mathbf{w}}_k + \beta_k\underline{\mathbf{v}}_k \end{aligned} \tag{2}$$

where the Kalman gain is given by

$$\mathbf{K}_k = \mathbf{P}_{k|k-1}\mathbf{C}^{\text{T}}(\mathbf{C}\mathbf{P}_{k|k-1}\mathbf{C}^{\text{T}} + \mathbf{R})^{-1}$$

and the system model is chosen as presented in section III-A. Under Assumption 1 and with an appropriately large choice of $\mathbf{P}_0$, $\psi_k, \alpha_k, \beta_k$ converge to their steady-state values $\psi_\infty, \alpha_\infty, \beta_\infty$ monotonically such that $\mathbf{P}_{k|k} = \text{E}\{\tilde{\underline{\mathbf{x}}}_k\tilde{\underline{\mathbf{x}}}_k^{\text{T}}\} > \text{E}\{\tilde{\underline{\mathbf{x}}}_{k+1}\tilde{\underline{\mathbf{x}}}_{k+1}^{\text{T}}\} = \mathbf{P}_{k+1|k+1}$ ([14], Theorem 2) due to the existence of a unique stabilizing solution of the corresponding discrete algebraic Riccati equation (DARE) ([15], Theorem 23).

IV. Event-based Estimation with Correlated Inputs

To pave the way for the extension to multisensor systems, two methods to deal with correlated input data in event-based estimation are presented: the event-based augmented state (EBAS) approach and event-based fast covariance intersection (EBFCI).

A. Event-based Augmented State Estimator

After introducing the noise terms of the smart sensors, the EBAS estimator can be developed. With the AS approach, correlated noise is represented as an additional state [9]. This can be understood as using a shaping filter to produce the correlated noise from a white noise source. The advantages of the method lie in the minimum mean squared error (MMSE)-optimal state estimation or fusion result, its simplicity and applicability to many scenarios. However, the computational burden is increased due to the growth of the state vector and estimation error covariance matrix, respectively. Additionally, due to the reformulation of the problem with zero measurement noise, singularities in the Kalman gain $\mathbf{K}_k$ can occur. While the first challenge has to be considered during the system design, the second problem is naturally mitigated by the use of event-based transmissions where the additional measurement noise $\mathbf{Z}$ is introduced in non-transmission instants.

Within this work, we examine the two types of correlated noise referring to the smart sensors presented in III-E. An augmented state space model (SSM)

$$\begin{aligned}\underline{\mathbf{x}}_{k+1}^a &= \mathbf{A}^a\underline{\mathbf{x}}_k^a + \underline{\mathbf{w}}_k^a\,, \\ \underline{\mathbf{y}}_k^a &= \mathbf{C}^a\hat{\underline{\mathbf{x}}}_k^a + \underline{\mathbf{v}}_k^a\end{aligned}$$

with $\underline{\mathbf{w}}^a \sim \mathcal{N}(\underline{0}, \mathbf{Q}^a)$, $\underline{\mathbf{v}}^a \sim \mathcal{N}(\underline{0}, \mathbf{R}^a)$ is derived for each of the sensors.

1) FIR Sensor: In case of the FIR sensor, all instances of the process and measurement noise up to the filter length m, $\underline{\mathbf{w}}_k^{\text{last}} = [(\underline{\mathbf{w}}_{k-1})^{\mathrm{T}}, \dots (\underline{\mathbf{w}}_{k-m})^{\mathrm{T}}]^{\mathrm{T}}$ and $\underline{\mathbf{v}}_k^{\text{last}} = [(\underline{\mathbf{v}}_k)^{\mathrm{T}}, \dots (\underline{\mathbf{v}}_{k-m})^{\mathrm{T}}]^{\mathrm{T}}$, need to be added to the state vector, leading to the matrices

$$\underline{\hat{\mathbf{x}}}_k^a = \begin{bmatrix} \underline{\hat{\mathbf{x}}}_k \\ \underline{\mathbf{w}}_k^{\text{last}} \\ \underline{\mathbf{v}}_k^{\text{last,S}} \end{bmatrix}, \quad \mathbf{A}^a = \begin{bmatrix} \mathbf{A} & & \\ & \mathbf{N}_w & \\ & & \mathbf{N}_v^{\mathrm{S}} \end{bmatrix},$$
$$\mathbf{Q}^a = \mathbf{B}^a \begin{bmatrix} \mathbf{Q} & \\ & \mathbf{R}^{\mathrm{S}} \end{bmatrix} (\mathbf{B}^a)^{\mathrm{T}},$$
$$\underline{\mathbf{y}}_k^a = \underline{\hat{\mathbf{x}}}_k^{\text{FIR, S}}, \quad \mathbf{C}^a = \begin{bmatrix} \mathbf{I}_{\mathbf{n_x}} & -\boldsymbol{\mathcal{U}}\boldsymbol{\mathcal{L}} & \boldsymbol{\mathcal{U}} \end{bmatrix}, \quad \mathbf{R}^a = \mathbf{0}_{n_x}$$

with

$$\mathbf{N}_w = \begin{bmatrix} \mathbf{0}_{n_x \times (m-2)\cdot n_x} & \mathbf{0}_{n_x} \\ \mathbf{I}_{(m-2)\cdot n_x} & \mathbf{0}_{(m-2)\cdot n_x \times n_x} \end{bmatrix},$$
$$\mathbf{N}_v^{\mathrm{S}} = \begin{bmatrix} \mathbf{0}_{n_y^{\mathrm{S}} \times (m-1)\cdot n_y^{\mathrm{S}}} & \mathbf{0}_{n_y^{\mathrm{S}}} \\ \mathbf{I}_{(m-1)\cdot n_y^{\mathrm{S}}} & \mathbf{0}_{(m-1)\cdot n_y^{\mathrm{S}} \times n_y^{\mathrm{S}}} \end{bmatrix},$$
$$\mathbf{B}^a = \left[\begin{array}{c|c} \begin{matrix} \mathbf{I}_{n_x} \\ \mathbf{I}_{n_x} \\ \mathbf{0}_{(m-2)\cdot n_x \times n_x} \end{matrix} & \mathbf{0}_{m\cdot n_x \times n_x} \\ \hline \mathbf{0}_{m\cdot n_y^{\mathrm{S}} \times n_y^{\mathrm{S}}} & \begin{matrix} \mathbf{I}_{n_y} \\ \mathbf{0}_{(m-1)\cdot n_y^{\mathrm{S}} \times n_y^{\mathrm{S}}} \end{matrix} \end{array}\right],$$

and $\boldsymbol{\mathcal{U}}, \boldsymbol{\mathcal{L}}$ as defined in [12], [13].

2) KF Sensor: Because of the recursive nature of the KF error (Eq. (2)), only one variable needs to be added to the state in case of a KF sensor, such that the matrices of the augmented SSM are given by

$$\underline{\hat{\mathbf{x}}}_k^a = \begin{bmatrix} \underline{\mathbf{x}}_{k+1} \\ \underline{\tilde{\mathbf{x}}}_{k+1}^{\mathrm{S}} \end{bmatrix}, \quad \mathbf{A}^a = \begin{bmatrix} \mathbf{A} & \\ & \psi^{\mathrm{S}} \end{bmatrix},$$
$$\mathbf{Q}^a = \mathbf{B}^a \cdot \begin{bmatrix} \mathbf{Q} & \\ & \mathbf{R}^{\mathrm{S}} \end{bmatrix} \cdot (\mathbf{B}^a)^{\mathrm{T}}, \quad \mathbf{B}^a = \begin{bmatrix} \mathbf{I}_{n_x} & \mathbf{0}_{n_x \times n_y^{\mathrm{S}}} \\ \alpha^{\mathrm{S}} & \beta^{\mathrm{S}} \end{bmatrix}$$
$$\underline{\mathbf{y}}_k^a = \underline{\hat{\mathbf{x}}}_k^{\text{KF, S}}, \quad \mathbf{C}^a = \begin{bmatrix} \mathbf{I}_{n_x} & \mathbf{I}_{n_x} \end{bmatrix}, \quad \mathbf{R}^a = \mathbf{0}_{n_x}.$$

The superscript S marks quantities of individual sensors. The augmented SSMs can be used with the event-based estimator presented in III-C.

B. Event-based Fast Covariance Intersection

The second algorithm based on FCI [11] does not use any information about the correlation structure between estimates. Since EBFCI is independent of the network topology, the multisensor version is directly provided. Using the independence of $\mathbf{Z}$ (Theorem 1), an event-based adaptation of FCI for the fusion of estimates determined by sensors $i = 1, \dots, N$,

$$\omega^i = \frac{(\mathrm{tr}\{\bar{\mathbf{P}}_k^i\})^{-1}}{\sum_{i=1}^{N} (\mathrm{tr}\{\bar{\mathbf{P}}_k^i\})^{-1}},$$
$$\mathbf{P}_k = \left(\sum_{i=1}^{N} (\omega^i (\bar{\mathbf{P}}_k^i)^{-1}) \right)^{-1},$$
$$\underline{\hat{\mathbf{x}}}_k = \mathbf{P}_k \cdot \sum_{i=1}^{N} \omega^i (\bar{\mathbf{P}}_k^i)^{-1} \underline{\bar{\mathbf{x}}}_k^i,$$

is proposed. For the transmission variable $\gamma_k^i = 1$, $\underline{\bar{\mathbf{x}}}_k^i = \underline{\hat{\mathbf{x}}}_k^i$ and $\bar{\mathbf{P}}_k^i = \mathbf{P}_k^i$ are the estimate and the estimation error covariance received from node i. For $\gamma_k^i = 0$, $\underline{\bar{\mathbf{x}}}_k^i = \underline{c}_k^i$ and $\bar{\mathbf{P}}_k^i = \mathbf{P}_{\max}^i + \mathbf{Z}^i$ are used, where a conservative $\mathbf{P}_{\max}^i$ needs to be determined such that it reflects the maximum covariance of node i under the assumption that none of its predecessors (if applicable) has transmitted. For one sensor and one fusion center only, $\bar{\mathbf{P}}_k^{\mathrm{S}}$, $\mathbf{P}_{k|k-1}$ and $\underline{\bar{\mathbf{x}}}_k^{\mathrm{S}}$, $\underline{\hat{\mathbf{x}}}_{k|k-1}$ are fused.

While the EBFCI is already provided in a form that allows the fusion of multiple sensor estimates in arbitrary topology, the application of the presented EBAS approach shall be investigated in two different network topologies.

V. Event-based Multisensor Fusion

In the following, sensor networks with multiple smart sensors and one or multiple fusion centers are considered. Each smart sensor acts individually; as depicted in Fig. 1, each has its own triggering unit with an individual triggering condition. Every sensor observes the state of the same physical process fully or partially. The estimation results of the sensors are sent to the fusion centers through a wireless network in an event-based fashion. The capacity of the communications network is assumed to be sufficient to support event transmissions of all sensors at the same time. Two different topologies, a star and a chain topology as depicted in Fig. 2 and 3, are investigated, that jointly cover a wide variety of sensor network topologies.

A. Star Topology

The star topology depicted in Fig. 2 represents the fusion of multiple sensor estimates at one receiving node. The sensors can be heterogeneous and of one of the two types described in III-E. To extend the EBAS estimator to the case with multiple sensor inputs, depending on the sensor type, one or more variables have to be added to the state equation according to IV-A. In case of FIR sensors, identical instances of the process noise are only added to the state once. An exemplary SSM for one FIR and one KF sensor is

$$\begin{bmatrix} \underline{\mathbf{x}}_{k+1} \\ \underline{\mathbf{w}}_{k+1}^{\text{last}} \\ \underline{\mathbf{v}}_{k+1}^{\text{last,FIR}} \\ \underline{\tilde{\mathbf{x}}}_{k+1}^{\text{KF}} \end{bmatrix} = \begin{bmatrix} \mathbf{A} & & & \\ & \mathbf{N}_w & & \\ & & \mathbf{N}_v^{\text{FIR}} & \\ & & & \psi^{\text{KF}} \end{bmatrix} \begin{bmatrix} \underline{\mathbf{x}}_k \\ \underline{\mathbf{w}}_k^{\text{last}} \\ \underline{\mathbf{v}}_k^{\text{last,FIR}} \\ \underline{\tilde{\mathbf{x}}}_k^{\text{KF}} \end{bmatrix} +$$
$$\begin{bmatrix} \begin{matrix} \mathbf{I}_{n_x} \\ \mathbf{I}_{n_x} \\ \mathbf{0}_{(m-2)\cdot n_x \times n_x} \end{matrix} & & \\ & \begin{bmatrix} \mathbf{I}_{n_y^{\text{FIR}}} \\ \mathbf{0}_{(m-1)\cdot n_y^{\text{FIR}} \times n_y^{\text{FIR}}} \end{bmatrix} & \\ \alpha^{\text{KF}} & & \beta^{\text{KF}} \end{bmatrix} \begin{bmatrix} \underline{\mathbf{w}}_k \\ \underline{\mathbf{v}}_{k+1}^{\text{FIR}} \\ \underline{\mathbf{v}}_{k+1}^{\text{KF}} \end{bmatrix},$$
$$\underline{\mathbf{y}}_k^a = \begin{bmatrix} \mathbf{I}_{n_x} & -\boldsymbol{\mathcal{U}}\boldsymbol{\mathcal{L}} & \boldsymbol{\mathcal{U}} & \mathbf{I}_{n_x} \end{bmatrix} \begin{bmatrix} \underline{\mathbf{x}}_k \\ \underline{\mathbf{w}}_k^{\text{last}} \\ \underline{\mathbf{v}}_k^{\text{last,FIR}} \\ \underline{\tilde{\mathbf{x}}}_k^{\text{KF}} \end{bmatrix}.$$

If steady-state KF or FIR sensors are employed, an MMSE-optimal fusion at the fusion center w. r. t. the raw sensor measurements is possible using the AS approach, if transmissions

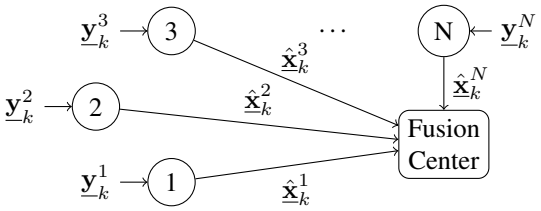

Fig. 2: Star Topology

of local estimates occur periodically at the same rate as the raw measurements are acquired at the sensors. In case of event-based transmissions the result is optimal w. r. t. the provided explicit and implicit information.

B. Chain Topology

As a second topology, a chain of nodes (Fig. 3), where the underlying graph is direct and acyclic and each node contains a KF to estimate the state of the observed system, is considered. This refers to using smart KF sensors as described in III-E2 in every node to enable optimal estimation and fusion. The chain topology is more challenging, since the state and estimation error of each node's estimator depend on all previous nodes and their correlations and event history. The goal is to decouple the chain, such that each node depends only on its direct predecessor. To achieve this, the AS approach comes into use and shows its potential. Using a naive approach would lead to adding all error states of all predecessors in the system to a node's SSM. However, this would imply a dependence of the computational costs on the chain length and would render the computations infeasible for long chains. A methodology to overcome this will be presented in the following.

1) Periodic Transmissions: Before looking into event-based transmissions, the system with chain topology will be examined under periodic transmissions between consecutive nodes at the same rate.

First, it will be shown how the error state of node i in the chain can be represented without depending on all error states of previous nodes with the help of an equivalent standard KF.

Lemma 1. Consider a chain of nodes as described in V-B and let all local measurements be processed at the rate they are acquired. Then, the error state equation of an arbitrary node i in the chain can be represented by the error state equation of an equivalent standard KF that processes all raw measurements $\underline{\mathbf{y}}^{1:i} = \left[(\underline{\mathbf{y}}^1)^{\mathrm{T}}, \ldots, (\underline{\mathbf{y}}^i)^{\mathrm{T}}\right]^{\mathrm{T}}$ acquired and used by nodes $1, \ldots, i$. If this equivalent error state equation is used in the augmented SSM of node $i+1$ according to IV-A2, the MMSE-optimal estimation result can be obtained.

Proof. The validity of the claim follows from the optimality of the AS approach [9]. If the estimation with the AS approach gives the MMSE-optimal result w. r. t. the raw measurements used in the local estimators, this is the same result obtained with a standard KF with the same measurements. Hence, it needs to be ensured that the fusion with the AS approach is optimal for one sensor (node i) and one fusion node (node $i+1$). This is done by investigating the propagation of the

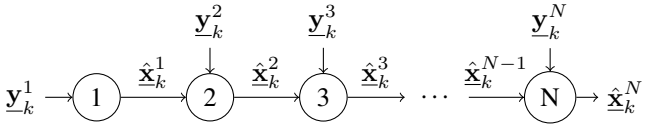

Fig. 3: Chain Topology

estimation error covariances, the propagation of the estimates follows analogously. The augmented SSM is given by

$$\begin{aligned}\begin{bmatrix}\underline{\mathbf{x}}_{k+1}^{i+1}\\ \tilde{\underline{\mathbf{x}}}_{k+1}^{i}\end{bmatrix} &= \begin{bmatrix}\mathbf{A} & \mathbf{0}_{n_x}\\ \mathbf{0}_{n_x} & (\mathbf{I}_{n_x} - \mathbf{K}_k^{\mathrm{i,KF}}\mathbf{C}^{1:i})\mathbf{A}\end{bmatrix}\begin{bmatrix}\underline{\mathbf{x}}_k^{i+1}\\ \tilde{\underline{\mathbf{x}}}_k^{i}\end{bmatrix}\\ &\quad + \begin{bmatrix}\mathbf{I}_{n_x} & \mathbf{0}_{n_x\times n_y^{1:i}}\\ -(\mathbf{I}_{n_x} - \mathbf{K}_k^{\mathrm{i,KF}}\mathbf{C}^{1:i}) & \mathbf{K}_k^{\mathrm{i,KF}}\end{bmatrix}\begin{bmatrix}\underline{\mathbf{w}}_k\\ \underline{\mathbf{v}}_{k+1}^{1:i}\end{bmatrix},\\ \underline{\mathbf{y}}_k^{i,a} &= \begin{bmatrix}\mathbf{I}_{n_x} & \mathbf{I}_{n_x}\end{bmatrix}\begin{bmatrix}\underline{\mathbf{x}}_k^{i+1}\\ \tilde{\underline{\mathbf{x}}}_k^{i}\end{bmatrix}\end{aligned}$$

with $\tilde{\underline{\mathbf{x}}}_k^i = \tilde{\underline{\mathbf{x}}}_k^{\mathrm{i,KF}}$ and $\underline{\mathbf{v}}^{1:i} = \left[(\underline{\mathbf{v}}^1)^{\mathrm{T}}, \ldots, (\underline{\mathbf{v}}^i)^{\mathrm{T}}\right]^{\mathrm{T}}$, $\mathbf{C}^{1:i} = \left[(\mathbf{C}^1)^{\mathrm{T}}, \ldots, (\mathbf{C}^i)^{\mathrm{T}}\right]^{\mathrm{T}}$. Let $\mathbf{P}_k = \begin{bmatrix}\mathbf{P}_k^{i+1,i+1} & \mathbf{P}_k^{i,i+1}\\ \mathbf{P}_k^{i,i+1} & \mathbf{P}_k^{i,i}\end{bmatrix}$ with $\mathbf{P}_k^{\mathrm{i,KF}} = \mathbf{P}_k^{i+1,i+1} = \mathbf{P}_k^{i,i} = -\mathbf{P}_k^{i+1,i} = -\mathbf{P}_k^{i,i+1}$ be the estimation error covariance at time step k. Then, using the KF prediction and update step, one finds after rearranging terms that $\mathbf{P}_{k+1}^{i+1,i+1} = \mathbf{P}_{k+1}^{\mathrm{i,KF}} = \mathbf{P}_{k+1}^{i,i} = -\mathbf{P}_{k+1}^{i+1,i} = -\mathbf{P}_{k+1}^{i,i+1}$ holds for $k+1$, which proves the optimal fusion $\forall k, \forall i$. Raw measurement of node 2 are added to both estimates equally. □

Furthermore, to avoid having to share information about the raw sensor measurements with all subsequent nodes to determine the equivalent error state equations, the measurements are combined to an artificial measurement vector with a maximum dimension of the state vector. This is done using the information form of the KF, where the information vector $\underline{\mathbf{i}}_{k|k-1}$ is updated with N independent measurements as

$$\underline{\mathbf{i}}_{k|k} = \underline{\mathbf{i}}_{k|k-1} + \sum_{i=1}^{N}(\mathbf{C}^i)^{\mathrm{T}}(\mathbf{R}^i)^{-1}\underline{\mathbf{y}}_k^i\,.$$

We define

$$\boldsymbol{\mathcal{Y}}_k = \begin{bmatrix}\underline{\mathbf{y}}_k^1\\ \vdots\\ \underline{\mathbf{y}}_k^N\end{bmatrix}, \quad \boldsymbol{\mathcal{C}} = \begin{bmatrix}\mathbf{C}^1\\ \vdots\\ \mathbf{C}^N\end{bmatrix}, \quad \boldsymbol{\mathcal{R}} = \begin{bmatrix}\mathbf{R}^1 & & \\ & \ddots & \\ & & \mathbf{R}^N\end{bmatrix}$$

to write the equation as a batch update instead of a sequential update with multiple independent measurements, i. e., $\underline{\mathbf{y}}_k, \mathbf{C}, \mathbf{R}$ are replaced by $\boldsymbol{\mathcal{Y}}_k, \boldsymbol{\mathcal{C}}, \boldsymbol{\mathcal{R}}$. It follows

$$\begin{aligned}\underline{\mathbf{i}}_{k|k} &= \underline{\mathbf{i}}_{k|k-1} + \boldsymbol{\mathcal{C}}^{\mathrm{T}}\boldsymbol{\mathcal{R}}^{-1}\boldsymbol{\mathcal{Y}}_k\\ &= \underline{\mathbf{i}}_{k|k-1} + \boldsymbol{\mathcal{C}}^{\mathrm{T}}\boldsymbol{\mathcal{R}}^{-1}\boldsymbol{\mathcal{C}}(\boldsymbol{\mathcal{C}}^{\mathrm{T}}\boldsymbol{\mathcal{R}}^{-1}\boldsymbol{\mathcal{C}})^{-1}\boldsymbol{\mathcal{C}}^{\mathrm{T}}\boldsymbol{\mathcal{R}}^{-1}\boldsymbol{\mathcal{Y}}_k\\ &= \underline{\mathbf{i}}_{k|k-1} + \bar{\mathbf{C}}^{\mathrm{T}}\bar{\mathbf{R}}^{-1}\bar{\underline{\mathbf{y}}}_k\,,\end{aligned}$$

with the new averaged measurement

$$\bar{\underline{\mathbf{y}}}_k = (\boldsymbol{\mathcal{C}}^{\mathrm{T}}\boldsymbol{\mathcal{R}}^{-1}\boldsymbol{\mathcal{C}})^{-1}\boldsymbol{\mathcal{C}}^{\mathrm{T}}\boldsymbol{\mathcal{R}}^{-1}\boldsymbol{\mathcal{Y}}_k\,. \tag{3}$$

Hence, the new measurement $\bar{\underline{\mathbf{y}}}_k$ can be obtained using a weighted least squares (WLS) estimator without altering the estimation result of the KF. It has the variance $\bar{\mathbf{R}} = \boldsymbol{\mathcal{C}}^{\mathrm{T}}\boldsymbol{\mathcal{R}}^{-1}\boldsymbol{\mathcal{C}}$

and the measurement matrix $\bar{\mathbf{C}}$ is given by the identity for all observable states and zero elsewise. To ensure full rank of $\mathcal{C}^{\mathrm{T}}\mathcal{R}^{-1}\mathcal{C}$, unobserved states need to be removed before applying the fusion rule (3). To preserve the original structure of the state, they have to be added again to $\bar{\mathbf{R}}$, $\bar{\mathbf{C}}$.

Now, the previous findings can be combined to formulate decoupled error state equations in the chain topology.

Theorem 2. Let every node in the chain employ a steady-state KF with $\mathbf{K}_k^i = \mathbf{K}_\infty^i$ and the measurements of previous nodes be combined iteratively according to Eq. (3) resulting in a new measurement noise $\bar{\underline{\mathbf{v}}}_k^{i-1} \sim \mathcal{N}\left(0, \bar{\mathbf{R}}^{i-1}\right)$. Then, the augmented SSM can be formulated as

$$\begin{bmatrix} \underline{\mathbf{x}}_{k+1} \\ \tilde{\underline{\mathbf{x}}}_{k+1}^{i-1} \end{bmatrix} = \begin{bmatrix} \mathbf{A} & \mathbf{0}_{n_x} \\ \mathbf{0}_{n_x} & \psi_\infty^{i-1} \end{bmatrix} \begin{bmatrix} \underline{\mathbf{x}}_k \\ \tilde{\underline{\mathbf{x}}}_k^{i-1} \end{bmatrix} + \begin{bmatrix} \mathbf{I}_{n_x} & \mathbf{0}_{n_x \times n_y} \\ \alpha_\infty^{i-1} & \beta_\infty^{i-1} \end{bmatrix} \begin{bmatrix} \underline{\mathbf{w}}_k \\ \bar{\underline{\mathbf{v}}}_{k+1}^{i-1} \end{bmatrix},$$

$$\underline{\mathbf{y}}_k^{i,a} = \begin{bmatrix} \mathbf{I}_{n_x} & \mathbf{I}_{n_x} \\ \mathbf{C}^i & \mathbf{0}_{n_x} \end{bmatrix} \begin{bmatrix} \underline{\mathbf{x}}_k \\ \tilde{\underline{\mathbf{x}}}_k^{i-1} \end{bmatrix} + \begin{bmatrix} \mathbf{0}_{n_x} \\ \underline{\mathbf{v}}_k^i \end{bmatrix}$$

for $i = 2, \ldots, N$ using the error state equation of a standard KF and the definitions in Eq. (2). The MMSE-optimal estimation result $\hat{\underline{\mathbf{x}}}_k^i$ can be obtained using a standard KF.

Proof. The error of a steady-state KF can be represented by Eq. (2). Since a steady-state KF with $\mathbf{K}_k^i = \mathbf{K}_\infty^i$ is used, $\psi_k^i = \psi_\infty^i$, $\alpha_k^i = \alpha_\infty^i$, $\beta_k^i = \beta_\infty^i$ hold. The results of Lemma 1 allow using the error state equation of a standard KF that processes all sensor measurements $\underline{\mathbf{y}}_k^1, \ldots, \underline{\mathbf{y}}_k^{i-1}$ to represent the estimation error of node $i-1$ in the chain. Finally, the sensor measurements $i = 1, \ldots, N$ can be combined to $\bar{\underline{\mathbf{y}}}_k^{i-1}$ using Eq. (3). Hence, the given augmented SSM is valid for any node $i = 2, \ldots, N$ and the MMSE result regarding the measurements $\underline{\mathbf{y}}_k^1, \ldots, \underline{\mathbf{y}}_k^i$ is obtained if used with a standard KF at node i. □

For time invariant systems satisfying assumption 1, $\psi_k^{i-1}, \alpha_k^{i-1}, \beta_k^{i-1}$ monotonically converge to constant values according to section III-E2. These quantities and $\bar{\mathbf{R}}^{i-1}, \bar{\mathbf{C}}^{i-1}$ have to be transmitted to all directly subsequent nodes, which can use them to calculate their own $\psi^i, \alpha^i, \beta^i, \bar{\mathbf{R}}^i, \bar{\mathbf{C}}^i$.

Theorem 2 provides a method to summarize all previous error terms in the error term of the preceding node $i-1$ and hence the goal stated in the beginning of the section is achieved. In the next section, an extension of the results to event-based transmissions will be discussed.

2) Event-based Transmissions: In case of event-based transmissions, the system is not in a steady state due to the switching measurement models in event/non-event instants. Hence, the considerations made for periodic transmissions are not admissible. In particular, the error state of a node depends on the event sequence of all of its preceding nodes. Knowledge of this event sequence and the full network topology is not assumed, as it would increase the amount of transmitted data and the computational complexity heavily. To ensure conservative estimation results, $\psi, \alpha, \beta, \bar{\mathbf{R}}, \bar{\mathbf{C}}$ have to be determined such that the accumulated real error of the respective node is bounded from above by the resulting error state.

Under the assumption that each node performs a state measurement itself, a valid upper bound can be obtained by omitting all previous measurements and only using the measurements of the respective sensor. This implies

$$\bar{\underline{\mathbf{v}}}_k^{i-1} = \underline{\mathbf{v}}_k^{i-1}, \quad \bar{\mathbf{R}}^{i-1} = \mathbf{R}^{i-1}, \bar{\mathbf{C}}^{i-1} = \mathbf{C}^{i-1},$$

which are used to determine $\psi^{i-1}, \alpha^{i-1}, \beta^{i-1}$. The parameters are altogether transmitted to the subsequent node to be used in the augmented SSM. The validity of this bound follows from the fact that including an additional measurement in Eq. (3) never worsens the performance due to

$$\left(\mathbf{C}_1^{\mathrm{T}}\mathbf{R}_1^{-1}\mathbf{C}_1 + \mathbf{C}_2^{\mathrm{T}}\mathbf{R}_2^{-1}\mathbf{C}_2\right)^{-1} \leq \mathbf{C}_1^{\mathrm{T}}\mathbf{R}_1\mathbf{C}_1\,,\ \mathbf{C}_2^{\mathrm{T}}\mathbf{R}_2\mathbf{C}_2\,.$$

An advantageous property of this upper bound is that in case of changing network topologies the error state of a node needs to be updated only if the directly preceding node is affected.

VI. Simulation Results

To evaluate the performance of the presented EBAS and EBFCI approaches in star and in chain topology, Monte Carlo simulations with 1000 runs are used.

A. System Model

As a system model, a nearly-constant velocity model in 1-D is considered. The matrices of the state equation are given by

$$\mathbf{A} = \begin{bmatrix} 1 & \Delta \\ 0 & 1 \end{bmatrix}, \quad \mathbf{Q} = \begin{bmatrix} \Delta^3/3 & \Delta^2/2 \\ \Delta^2/2 & \Delta \end{bmatrix},$$

where $\Delta = 0.3$ is the sampling interval. All nodes use the same $\mathbf{Z}$ in their triggering unit. A standard KF, that receives all raw sensor measurements periodically and achieves the MMSE-optimal result, is used for comparison.

B. Star Topology

A network of four heterogeneous smart sensors transmitting to a fusion center is investigated. The fusion center does not acquire measurements through a measurement unit itself. Two steady-state KF sensors and two FIR sensors are used. Their measurement models are $\mathbf{C}^1 = \begin{bmatrix} 1 & 1 \end{bmatrix}$, $\mathbf{R}^1 = 3$ and $\mathbf{C}^{2,3,4} = \begin{bmatrix} 1 & 0 \end{bmatrix}$, $\mathbf{R}^{2,3,4} = 1$. The FIR sensors use filter lengths of $m^3 = 5$, $m^4 = 2$. First, the optimal Kalman gain for $k \to \infty$ is set for both KF sensors. The results are shown in Fig. 4, where the mean squared error (MSE) is plotted over the mean communication rate per sensor. As expected, EBFCI is an upper bound for EBAS for all communication rates since FCI does not use correlation information. For high communication rates, EBAS approaches the MMSE result.

In the second scenario, a suboptimal Kalman gain of $\mathbf{K} = 0.25 \cdot \mathbf{K}_\infty$ is used at the two KF sensors. As seen in Fig. 5, while the results for EBAS remain almost unchanged, the performance of FCI worsens significantly due to the ignorance of the correlation structure. From this example it can be seen clearly that the performance of EBAS does not depend on the performance of the estimators located in the smart sensors. The MMSE-optimal result is always obtained for periodic transmissions. However, the performance of the smart sensors' estimators influence their transmission frequency.

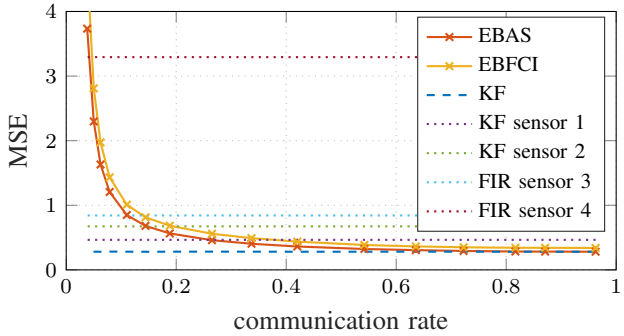

Fig. 4: Two KF and two FIR sensors in star topology. The KF sensors use the steady-state gain of $\mathbf{K} = \mathbf{K}_\infty$.

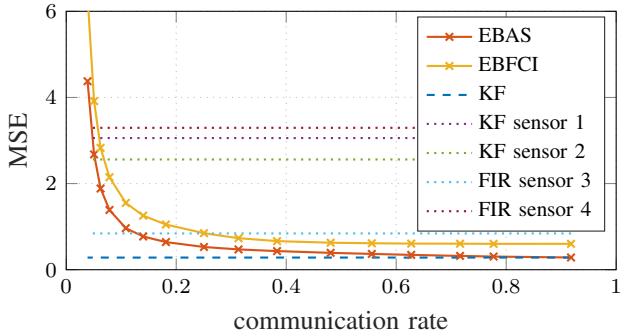

Fig. 5: Two KF and two FIR sensors in star topology. The KF sensors use a steady-state gain of $\mathbf{K} = 0.25 \cdot \mathbf{K}_\infty$.

C. Chain Topology

A chain of seven nodes, each equipped with a sensor to measure the system state ($\mathbf{C}^i = \begin{bmatrix}1 & 0\end{bmatrix}$, $\mathbf{R}^i = 1, i = 1, \ldots, 7$) and an estimator to fuse the predecessor's state and the obtained measurement, is considered for the simulation of the chain topology.

1) Periodic transmissions: The setup presented in section V-B1 is used to evaluate the performance of AS and FCI in chain topology. The average MSE per time step for sensor 7 is plotted in Fig. 6 for AS, FCI and KF. The curves of the developed AS and the standard KF coincide as expected and AS achieves the MMSE-optimal result. The MSE of FCI is worse over all time steps due to the unconsidered correlations.

2) Event-based transmissions: To evaluate the system under event-based transmissions, the setup described in V-B2 is used. In Fig. 7, it is visible that EBAS (solid lines) does not always perform significantly better than EBFCI (dotted lines). Taking a closer look, all three curves overlap for sensor 1, which is reasonable, since no fusion takes place. The curve of EBAS approaches KF (dashed lines) for sensor 2 due to the correct error assumption in this case and EBAS being MMSE-optimal for a communication rate of 1. EBFCI performs worse than EBAS for sensors 2-4 for all communication rates. However, for sensors 5-7 the curves of EBAS and EBFCI approach each other for high communication rates. This is due to the fact that the error bound determined in V-B2 is conservative.

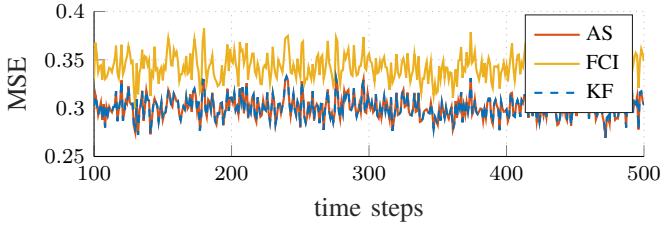

Fig. 6: Average MSE of sensor 7 per time step

For low communication rates, all curves approach the MSE that is obtained with a single measurement equal to sensor 1.

3) Average transmission rate per time step: To assess the communications resource utilization, the average transmission rate of the whole network is analyzed. While one available channel per sensor is assumed in this work, in real world applications it would be desirable to allocate less for low communication rates. However, this is only possible, if the events are well distributed, i. e., uniformly over time, and the system can tolerate a certain amount of packet losses due to collisions. To evaluate the distribution of the events, a histogram of the events triggered for a transmission rate of approximately 0.5 ($\mathbf{Z} = \left[\begin{smallmatrix}0.1 & 0\\ 0 & 1\end{smallmatrix}\right]$) is plotted in Fig. 8. As desired, the distribution is approximately Gaussian with a mean of 3.57 events per time step. This indicates that the event distributions of the individual nodes in the chain are independent of each other.

VII. Conclusions

In this paper, event-based multisensor fusion with correlated estimates in two different topologies, namely the star and the chain topology, was investigated. To enable this, the EBAS approach was developed as well as an event-based extension of FCI. While the EBAS approach leads to the MMSE-optimal result in case of periodic transmissions, EBFCI provides a suboptimal solution in any case. In star topology, two different smart sensor types were investigated, FIR and KF sensors. The simulation of suboptimal KF sensors shows that EBAS maintains its optimal result while EBFCI's performance degrades. In chain topology, for periodic transmissions an MMSE-optimal and resource-efficient method was developed for EBAS, while with event-based transmissions, only suboptimal solutions are possible due to the unknown event sequence of previous nodes. An admissible error bound for the error of previous nodes was found for both, EBAS and EBFCI. However, especially in the case of EBAS, the bound is conservative and leads to EBFCI performing similarly as EBAS for high communication rates in chain topology. Accordingly, EBFCI could be chosen for high communication rates smaller than one. Nevertheless, in contrast to EBAS, it has to be taken into account that EBFCI requires the transmission of $\mathbf{P}_k^i$ in addition to $\underline{\hat{\mathbf{x}}}_k^i$ in transmission instances.

Hence, in the future, tighter error bounds for the EBAS approach in chain topology shall be found as well as a bound if the considered node does not obtain measurements itself (i. e., a node that fuses multiple chains). Furthermore,

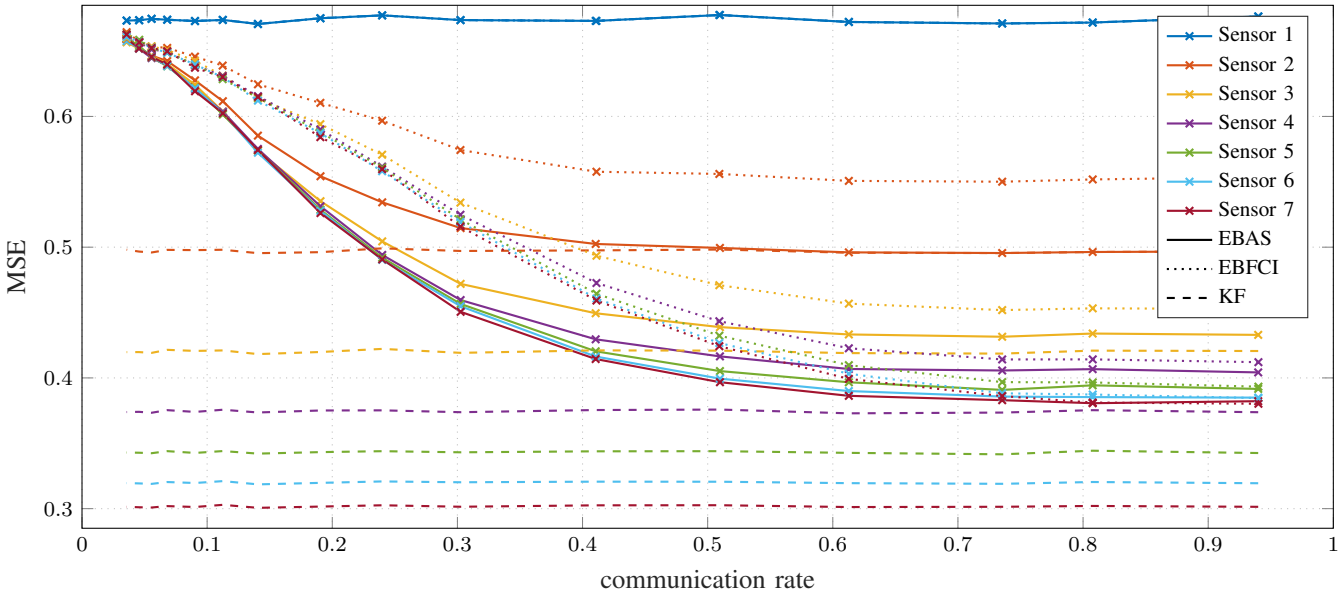

Fig. 7: Chain of seven sensors with event-based transmissions with varying $\mathbf{Z}$.

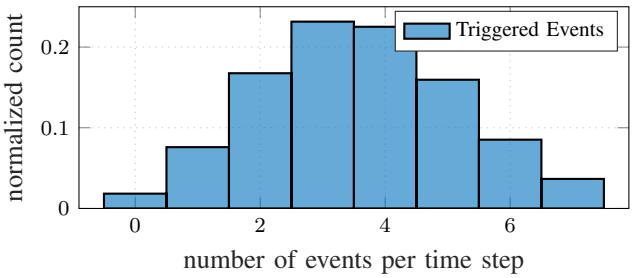

Fig. 8: Histogram of the event distribution per time step in the network for a communication rate of 0.5 using EBAS.

the measurement combination rule in (3) assumes that all measurements are acquired and processed simultaneously. An adaptation of this rule is required for asynchronous acquisition and sequential processing. To allow for less assigned channels than communication links, strategies to handle packet losses induced by collisions need to be developed. Finally, to allow for an easy system design, an analytical solution to determine the communication rate depending on $\mathbf{Z}$ shall be found.

Acknowledgment

This work was partially funded by the Deutsche Forschungsgemeinschaft (DFG, German Research Foundation) under project number 515674308.

References

[1] W. Dargie and C. Poellabauer, *Fundamentals of Wireless Sensor Networks*. John Wiley & Sons, Oct. 2010.

[2] M. Majid, S. Habib, A. Javed, M. Rizwan, G. Srivastava, T. Gadekallu, and J.-W. Lin, "Applications of Wireless Sensor Networks and Internet of Things Frameworks in the Industry Revolution 4.0: A Systematic Literature Review," *Sensors*, no. 6, 2022.

[3] D. Han, Y. Mo, J. Wu, S. Weerakkody, B. Sinopoli, and L. Shi, "Stochastic Event-Triggered Sensor Schedule for Remote State Estimation," *IEEE Transactions on Automatic Control*, vol. 60, no. 10, pp. 2661–2675, Oct. 2015.

[4] M. T. Andren and A. Cervin, "Event-Based State Estimation Using an Improved Stochastic Send-on-Delta Sampling Scheme," in *2016 Second International Conference on Event-based Control, Communication, and Signal Processing (EBCCSP)*. IEEE, Jun. 2016.

[5] E. J. Schmitt, B. Noack, W. Krippner, and U. D. Hanebeck, "Gaussianity-Preserving Event-Based State Estimation With an FIR-Based Stochastic Trigger," *IEEE Control Systems Letters*, vol. 3, no. 3, pp. 769–774, Jul. 2019.

[6] R. Forsling, B. Noack, and G. Hendeby, "A Quarter-Century of Covariance Intersection: Correlations Still Unknown? (to appear)," *IEEE Control Systems Magazine*, Apr. 2024.

[7] Y. Bar-Shalom and L. Campo, "The Effect of the Common Process Noise on the Two-Sensor Fused-Track Covariance," *IEEE Transactions on Aerospace and Electronic Systems*, vol. AES-22, no. 6, pp. 803–805, Nov. 1986.

[8] C.-Y. Chong, S. Mori, F. Govaers, and W. Koch, "Comparison of Tracklet Fusion and Distributed Kalman Filter for Track Fusion," in *Proceedings of the 17th International Conference on Information Fusion (Fusion 2014)*, 2014, pp. 1–8.

[9] A. E. Bryson and L. J. Henrikson, "Estimation Using Sampled-Data Containing Sequentialty Correlated Noise," *Journal of Spacecraft and Rockets*, vol. 5, no. 6, 1968.

[10] P. Jiang, J. Zhou, and Y. Zhu, "Globally Optimal Kalman Filtering with Finite-Time Correlated Noises," in *49th IEEE Conference on Decision and Control (CDC)*, Atlanta, GA, USA, Dec. 2010, pp. 5007–5012.

[11] W. Niehsen, "Information Fusion Based on Fast Covariance Intersection Filtering," in *Proceedings of the Fifth International Conference on Information Fusion (FUSION 2002)*, vol. 2. Annapolis, MD, USA: Int. Soc. Inf. Fusion, 2002, pp. 901–904.

[12] B. Noack, C. Öhl, and U. D. Hanebeck, "Event-Based Kalman Filtering Exploiting Correlated Trigger Information," in *Proceedings of the 25th International Conference on Information Fusion (Fusion 2022)*, Linköping, Sweden, Jul. 2022.

[13] E. J. Schmitt and B. Noack, "Event-based Colored-Noise Kalman Filtering for Improved Resource Efficiency," in *Proceedings of the combined IEEE 2023 Symposium Sensor Data Fusion and International Conference on Multisensor Fusion and Integration (SDF-MFI 2023)*, Bonn, Germany, Nov. 2023.

[14] R. R. Bitmead, M. R. Gevers, I. R. Petersen, and R. J. Kaye, "Monotonicity and Stabilizability properties of solutions of the Riccati difference equation: Propositions, lemmas, theorems, fallacious conjectures and counterexamples," *Systems and Control Letters*, vol. 5, no. 5, pp. 309–315, Apr. 1985.

[15] D. Simon, *Optimal State Estimation: Kalman, H [Infinity] and Nonlinear Approaches*. Hoboken, N.J: Wiley-Interscience, 2006.